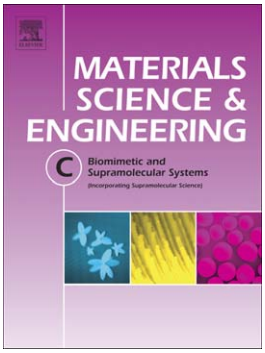

Comparison of a xenogeneic and an alloplastic material used in dental implants in terms of physico-chemical characteristics and *in vivo* inflammatory response

Andreia Figueiredo, Patrícia Coimbra, António Cabrita, Fernando Guerra, Margarida Figueiredo

PII: S0928-4931(13)00276-2
DOI: doi: 10.1016/j.msec.2013.04.047
Reference: MSC 4009

To appear in: *Materials Science & Engineering C*

Received date: 14 January 2013
Revised date: 18 April 2013
Accepted date: 22 April 2013

Please cite this article as: Andreia Figueiredo, Patrícia Coimbra, António Cabrita, Fernando Guerra, Margarida Figueiredo, Comparison of a xenogeneic and an alloplastic material used in dental implants in terms of physico-chemical characteristics and *in vivo* inflammatory response, *Materials Science & Engineering C* (2013), doi: 10.1016/j.msec.2013.04.047

Comparison of a xenogeneic and an alloplastic material used in dental implants in terms of physico-chemical characteristics and *in vivo* inflammatory response

Andreia Figueiredo[a,b,c], Patrícia Coimbra[d,*], António Cabrita[a], Fernando Guerra[b], Margarida Figueiredo[d´]

[a] Experimental Pathology Service, University of Coimbra, 3004-504 Coimbra, Portugal

[b] Dentistry Department, University of Coimbra, 3030-005 Coimbra, Portugal

[c] Catholic Portuguese University, Health Sciences Department, 3504-505 Viseu, Portugal

[d] Chemical Engineering Department, University of Coimbra, 3030-290 Coimbra, Portugal

*Corresponding author at: Department of Chemical Engineering, University of Coimbra, Polo II, 3030-790 Coimbra, Portugal. Tel.: +351 239798703; fax: +351 239798700.

E-mail address: patrícia@eq.uc.pt (P. Coimbra).

Abstract

Two commercial bone grafts used in dentistry (Osteobiol Gen-Os®, a xenograft of porcine origin, and Bonelike®, a hydroxyapatite based synthetic material), in the form of granules, were characterized and evaluated *in vivo* regarding the intensity of the tissue inflammatory response. These biomaterials were characterized in terms of morphology, particle size distribution, porosity and pore size, specific surface are and density. The chemical composition and structure of the materials were accessed by Fourier-Transform Infrared Spectroscopy (FTIR) and X-ray Diffraction (XRD). The graft materials were implanted in the *gluteus maximus* muscles of Wistar rats and the inflammatory response evaluated through histological analysis, after one week of implantation.

The results showed that the two grafts have quite different characteristics in practically all the evaluated properties. While Osteobiol® exhibits a structure and composition similar to the natural bone, Bonelike® is constituted by a main crystalline phase of hydroxyapatite and two secondary phases of α- and β-tricalcium phosphate. Osteobiol® granules, besides being larger, are irregular, and exhibit sharp-edged tips, while those of Bonelike® are approximately cylindrical, with round contours, and more uniform in size. The *in vivo* response evaluated from the inflammatory infiltrates revealed that although both implants did not cause severe inflammation, Bonelike® granules elicit a consistently more intense inflammatory reaction than that triggered by the granules of Osteobiol®, particularly in terms of collagen production and formation of fibrous capsule. This reaction was partly explained in terms of the characteristics evaluated for the granules of this material.

Keywords

Bone grafts, physico-chemical properties, inflammatory response

1. Introduction

Bone grafts are widely used in surgical procedures in Dentistry, particularly in Periodontology [1-5], Implantology [2, 6, 7], Endodontics [3, 5, 8-10] and Oral Surgery [11, 12]. Although autogeneous bone continues to be the "gold standard" in bone substitution [13-20], its limited availability and the need for a second surgical site and procedure drove the quest to other alternatives, like allografts (from cadavers), xenografts (from animals) and numerous synthetic materials [15-17, 20, 21], all having merits and limitations [13, 15].

Although many synthetic materials have been recently developed (with quite different chemical compositions and structural characteristics to suit many distinct applications), to date no synthetic material has been able to meet all desirable features: to match biological and mechanical properties of human bone [18]. In fact, synthetic grafts continue to have their limitations, being one of the most important the patient's immune response to a foreign substance and the possibility of reaction from the host. Inflammation, granulation tissue, foreign body reaction and fibrosis/fibrous capsule development are events that frequently occur [22]. Among their advantages is the fact that alloplastic materials are available in infinite supply and are relatively inexpensive, immunologically inert and completely sterile [19].

Concerning dentistry and maxillofacial surgery, xenogeneic grafting has been one of the most popular forms of bone grafting followed by alloplastic graft materials [23]. Moreover, in the daily clinic, xenografts are often used for the same indications as synthetic materials [13], being exclusively the dentist's choice to use one over the other. The ultimate decision is based on many factors, including the size and location of the bone tissue defect as well as the structural, biological and biomechanical properties of the graft itself [21]. However, the large number of alternatives available, in contrast

with the lack of reliable information regarding their indications and effectiveness, as well as comparative studies, leaves the choice of the grafting material to the surgeon´s preferences, not always scientifically based [16].

It has been shown that physico-chemical properties (like chemical composition and particle morphology) are among the most important factors that influence the material performance *in vivo*, causing significantly different biological responses [22, 24-27]. In fact, such properties may change the behavior of macrophages in processes like adhesion, apoptosis, fusion and cytokine secretion [28]. Hence, detailed information about graft material characteristics is absolutely crucial not only to choose the most appropriate materials but also to properly evaluate their clinical outcomes.

The present study compares two bone graft materials widely used by dentists - a xenograft (Osteobiol®) and a hydroxyapatite based synthetic material (Bonelike®) - in terms of chemical composition, crystallinity, particle size and size distribution, porosity, surface area and density. Additionally, the biological behavior of both materials was evaluated in *vivo* in terms of their inflammatory response after intramuscular injection in rats. This evaluation is most relevant since although xenogeneic and alloplastic materials have been extensively investigated, the tissue response to these bone substitutes has only been partially elucidated [29].

2. Materials and methods

Osteobiol® Gen-Os Mix (Tecnoss, Giaveno, Italy) is a xenograft of porcine origin, formed by hydroxyapatite (HA) and collagen type I, having 80% of cancellous bone and 20% of cortical bone. Due to the low processing temperature (130°C), this material is claimed to preserve the structure and composition of the natural bone components [30]. Bonelike® (Medmat Innovation, Porto, Portugal) is a synthetic bone substitute, being

formed by a patented glass-reinforced hydroxyapatite [31], prepared with the incorporation of a P_2O_5-based glass in the HA by means of a liquid phase sintering process [32, 33], allegedly to increase, simultaneously, the mechanical properties of HA and to introduce ions commonly found in bone tissue [34, 35]. According to the producers, Bonelike® is composed of a main crystalline phase of HA and two secondary phases of α- and β-tricalcium phosphate (TCP) [36].

Osteobiol® Gen-Os granules, with a reported size of 0.25 mm to 1.00 mm, and Bonelike® granules, with a reported particle size range between 0.25 mm and 0.5 mm, were characterized and used *in vivo* in the as-received form.

2.1. Physico-chemical characterization

Grafting material morphology was assessed by scanning electron microscopy (SEM) in a JEOL JSM 35C, by spreading a few granules on a double-sided carbon conductive tape. The granules were sputter-coated with gold and examined under an accelerating voltage of 10 kV. Additionally, energy dispersive X-ray spectroscopy (EDS) was used to find the overall approximate Ca/P ratio at three randomly selected spots.

Particle size distribution was determined by laser diffraction spectrometry in a Mastersizer 2000 (Malvern Instruments, UK). At least three measurements were performed for each sample. The equipment software automatically computes the average particle size distribution and the corresponding statistical parameters, with 0.95 confidence level.

Information regarding samples porosity and pore size distribution was obtained by mercury intrusion porosiometry (Poresizer 9320, Micromeritics Instrument Corp., Norcross, GA) in a pressure range between 0.05 atm and about 2000 atm (corresponding to a range of pore diameters between 400 μm and 0.006 μm,

respectively). The porosity was calculated as the ratio of the total volume of mercury intruded and the total sample volume (measured at the lowest intrusion pressure and that includes solid material and voids (i.e. interstices and open pores smaller than 400 μm)). Two samples of each material were analyzed by this technique. A third sample was additionally analyzed if the measured porosity values differed by more than 5%. It should be noted that this technique uses a relatively large amount of material (thus ensuring sample representativeness) that cannot be further used (as it will be mercury contaminated).

The particles real density (mass per volume of solid, excluding empty spaces) was determined by gas pycnometry (Accupyc 1330, Micromeritics Instrument Corp.), using Helium. At least 10 runs were performed for each sample, and at least three different samples were analyzed for each material.

Samples specific surface area was measured by the nitrogen adsorption technique (ASAP 2000, Micromeritics Instrument Corp.) using the BET method. The samples analyzed by this method were the same as those subjected to porosimetry. As mentioned, at least two independent samples were measured for each material using the same validation criteria.

For contact angle analysis, the materials were compressed into tablets with a manual hydraulic press. About 100 mg of granules were filled into a 8 mm die and compressed with a force of 100 bar applied for 30 s. Static contact angles were obtained using the sessile drop method with a Dataphysics OCA-20 contact angle analyzer (DataPhysics Instruments, Filderstadt, Germany). The contact angle value obtained for each material is the average of at least five independent measurements.

Information about chemical composition was obtained by Fourier-Transform Infrared Spectroscopy (FTIR). Spectra were recorded in the range of 400-4000 cm^{-1} using a

JASCO 4200 spectrometer operating in the transmission mode. The materials were mixed with KBr and compressed in the form of discs with a manual press. Data collection was performed with a 4 cm^{-1} spectral resolution and 32 scans, at room temperature.

X-ray diffraction patterns (XRD) were collected using an X-PERT diffractometer (Philips, Amsterdam, Netherlands) operating in the Bragg-Brentano configuration with Co-Ka radiation (λ =1.78897 Å). Spectra were recorded in the range of $10^o < 2\theta < 100^o$ with a step interval of 0.025º and a step time of 0.5 s. Identification of the phases was achieved by comparing the obtained diffraction patterns with those from the database provided by ICDD (International Centre for Diffraction Data).

2.2. In vivo evaluation

Fifteen male Wistar rats, twelve weeks old (from Charles River Laboratories, Spain), were bred, kept under standard conditions, and provided with water *ad libitum* at the Coimbra's University Laboratory Animal Unit, Coimbra, Portugal. The animals were randomly allocated to three experimental groups: G1 (Osteobiol®), G2 (Bonelike®) and G3 (sham - control group, injected with saline), each of them with five animals. The animals of G1 and G2 received the biomaterial granules and the control group underwent operation without biomaterial implantation, in order to classify the inflammatory response related to the implantation procedure *per se*.

After intraperitoneal anesthesia (10 ml of ketamine 10mg/ml (Ketalar®) with 2 ml of chlorpromazine 50mg/2ml (Largactil®)), disinfection of the operative region was made. For better identification, the injection sites were shaven. 5 mg of the biomaterial were implanted, in sterile conditions, in the *gluteus maximus* muscles of each rat, using sterilized syringes with 20-gauge needles. The bone graft materials were compressed in

the injection syringe, with no carrier, to be less traumatic to the animal and to minimize interference from other substances to the inflammatory response. The animals were sacrificed one week later by an overdose of ketamine and chlorpromazine. These experiments were approved by the University's Ethical Committee, in accordance to guideline 1005/92 from 23/10/1992, that regulates care for animal's experimental usage. Immediately after death, the biomaterials were explanted together with the surrounding peri-implant tissue and fixed in 4% formalin neutral buffer solution (pH 7.4) for 24 h for further histological analysis. Biopsies were decalcified in 10% Tris-buffered EDTA at 37° C for 3 days, and subsequently dehydrated in a series of alcohol solutions, with increasing concentrations. Paraffin embedding was performed and cuts were made with a microtome (Shandon Finesse 325 Microtome). Sections were stained with hematoxylin and eosin (H&E) and Tricromic Masson (TM).

Histological analysis was conducted by two independent investigators, using a conventional diagnostic microscope (Nikon Eclipse E200). The outcome of the tissue-biomaterial interface was evaluated by examination not only of the implantation bed, but also of the peri-implant tissue.

As inflammation is normally characterized by the presence of multiple types of cells, such as macrophages, monocytes and lymphocytes, plasma cells and multinucleated giant cells [37], a semi-quantitative methodology based on the total number of these cells per field was implemented [38] in order to grade the intensity of the inflammatory response triggered by both materials. In such way the inflammatory response is classified as mild if the number of inflammatory cell per field is inferior to 25, moderate, when the number of cells is between 25 and 125, or severe, when the number of inflammatory cells are superior to 125.

3. Results

3.1. Physico-chemical characterization

A general view of the shape and size of Osteobiol® and Bonelike® granules is given in Figure 1, while details of their surface morphology can be distinguished in Figures 2 and 3. The latter figures also include representative EDS spectra of both materials. SEM analysis reveals that Bonelike® particles are approximately cylindrical, round edged, with a smooth surface and nearly monodispersed. On the other hand, those of Osteobiol® are larger, highly irregular, sharp edged and polydispersed.

The surface chemical composition obtained through EDS analysis (Figures 2d and 3d)) shows the presence of multiple elements normally found in bone, being Ca and P the most prominent. The determined Ca/P ratios (in atomic %; average of three measurements performed in different sample spots) were of 1.35±0.07 for Osteobiol®, and 1.75±0.16 for Bonelike®.

The properties of the two materials, regarding particle size distribution, specific surface area, porosity, pore size distribution, and density, are summarized in Table 1.

The particle size distribution curves are illustrated in Figure 4, whereas Table 1 presents the size parameters in terms of median diameter (D_{50}) as well as particle size range, expressed by the 10% and 90% percentiles (D_{10} and D_{90}). These results show that the Osteobiol® particles are considerably larger than those of Bonelike® (672 µm and 326 µm median size, respectively), confirming the microscopic observations. Moreover, Osteobiol® size distribution is essentially monomodal while that of Bonelike® exhibits a secondary mode around 15 µm.

The specific surface area of the two materials was determined by N_2 adsorption. The values obtained using the BET methods are listed in Table 1. As shown, the specific

surface area of Osteobiol® is considerably higher than the one of Bonelike®, despite the smaller particle size of the Bonelike® granules.

Mercury intrusion porosimetry curves (cumulative intruded volume versus pore diameter) are depicted in Figure 5. The mercury intruded volume together with the porosity values are listed in Table 1. As it can be seen, values close to 50 % were determined for both samples. However, as also quantified in Table 1, most of this porosity relates to interparticle voids and not to the particles internal pores (only about 12 % of the total porosity corresponds to pores smaller than 10 μm).

The real density (also called absolute density) was determined by gas pycnometry (Table 1). The measured values seem to be consistent with the samples composition: in the case of Osteobiol®, is inferior to that of hydroxyapatite (3.16 g cm^{-3}) [39], as expected for a collagenated sample; as for Bonelike® particles, a smaller value than that of hydroxyapatite was also anticipated due to its constitution (α- and β-TCP as secondary phases with theoretical densities of 2.86 g cm^{-3} and 3.07 g cm^{-3}, respectively [40]).

The X-ray diffraction patterns of Bonelike® and Osteobiol® are represented in Figures 6a) and 6b), respectively. They were compared to the diffraction patterns of pure hydroxyapatite (JCPDS nº 09-432), α-TCP (JCPDS nº 29-0359) and β-TCP (JCPDS nº 86-1585) and the signalized peaks were assigned to these three phases.

The FTIR spectra of the two graft materials are illustrated in Figure 7. In the Bonelike® spectrum (Figure 7a) it is possible to identify the characteristic stretching bands of the phosphate group (PO_4^{3-}), present in both HA and TCP (ν_3 mode bands at 1089 and 1044 cm^{-1}, the ν_1 band at 968 cm^{-1}, the ν_4 bands at 600 cm^{-1} and 570 cm^{-1}, and the ν_2 band at 470 cm^{-1} [41, 42]). Also detectable are the weak bands assigned to the hydroxide ion (OH^-) in hydroxyapatite, appearing as a sharp peak at 3577 cm^{-1}

(stretching vibration) and at ~635 cm^{-1} (liberation band) [41, 42]. The broad band between 3600-3150 cm^{-1} corresponds to O-H stretching vibration in the water molecules present in the material. It is also interesting to note the presence of two low intensity bands in the region of the C-H stretching vibrations (2900-2800 cm^{-1}). This is probably originated by some impurities of organic nature. The presence of residual carbon as also been detected in the EDS spectrum of this material (Figure 2d).

As expected, the FTIR spectrum of Osteobiol® (Figure 7b) is very similar to the ones registered from porcine or human bone samples [39], displaying the typical bands of collagen (bands of amide I (~1660 cm^{-1}) and amide II (~1550 cm^{-1}) [41]) and of hydroxyapatite (the stretching vibrations of the PO_4^{3-} group). Contrary to that of Bonelike®, in this spectrum are also visible a few bands attributed to the stretching vibrations of the carbonate group (the ν_3 mode, appearing as a double band between 1400 cm^{-1} and 1500 cm^{-1}, and the ν_2 mode band at ~878 cm^{-1}), which reveals the carbonated (natural) structure of the hydroxyapatite present in this graft [43]. On the other hand, the vibrations bands of the OH^- are not detectable.

The hydrophilic/hydrophobic character of Osteobiol® and Bonelike® was, as described earlier, evaluated by measuring the water contact angle by the sessile drop method. For Bonelike®, a contact angle value of 26.7 ± 4.3˚ was obtained while for Osteobiol® the measured value was of 51.4 ± 7˚. These results indicate that both materials are hydrophilic.

3.2. In vivo evaluation

The tissue reaction for the sham group (injected with saline, G3) and for each experimental group (Osteobiol® (G1) and Bonelike® (G2)), one week after implantation, is illustrated by some representative micrographs of histological sections in Figures 8, 9 and 10, using hematoxylin and eosin (H&E) and Tricromic Masson

(TM) staining. No inflammation was found in the sham group (Figure 8), being only evident muscle fibers disrupted due to the injection procedure.

The inflammatory response to Osteobiol® implant (Figure 9) is characterized by the presence of a great number of lymphocytes. There is a discrete presence of polymorphonuclear leukocytes, as well as some inflammatory multinucleated giant cells. Additionally, some blood capillaries with red blood cells and some fibroblasts around the graft particles can be found. A capsule was formed in the outer limit of the graft and traces of collagen were also detected (green coloring in Fig 9b). According to the criteria adopted to classify the inflammatory response (described earlier in Materials and Methods), this can be considered as moderate (84 ± 7 inflammatory cells per field, average of ten measurements).

Bonelike® granules (Figure 10) deploy a more intense inflammatory response, but still moderate (112 ± 10 total inflammatory cells per field, average of ten measurements), with predominance of lymphocytes. The histological analysis also shows several multinucleated giant cells, few blood capillaries with red blood cells and some fibroblasts around the particles. However, in this case, the capsules surrounding the granules were thicker than those originated by Osteobiol®. Moreover, a more intense reaction regarding collagen was also found (Figure 10b).

For both biomaterials, however, there was no evidence of necrotizing reaction, nor important hemorrhage.

Additionally, the tissue reaction to the biomaterials implantation was assessed according to the reparative process characterization: degree of fibrosis and fibroblastic proliferation. Table 2 lists the scores obtained for the different parameters according to the criteria described, after careful examination of an average of 10 sections for each tissue sample. As seen in Figures 9b) and 10b) there is evidence of a more intense

fibrosis response, a higher content of collagen and a thicker capsule around the graft particles in Bonelike® samples, when compared to those of Osteobiol®.

4. Discussion

Although the *in vivo* response evaluated from inflammatory infiltrates (Figures 9 and 10) revealed that both implants did not cause severe inflammation, Bonelike® particles triggered a larger number of inflammatory cells and a lighter degree of fibrosis.

Despite different responses were somehow anticipated since these materials, as the results show, have quite distinct properties, the following discussion will try to interpret the *in vivo* inflammatory response of these two biomaterials in terms of their physical and chemical characteristics.

In fact, morphological data assessed by SEM revealed that these two materials are quite different in what concerns shape, surface topography and size (Figures 1, 2, 3 and 4). Osteobiol® particles, besides being larger (nearly double), are irregular and exhibit sharp-edged tips (reflecting the natural origin of this material, constituted by fragments of cancellous and cortical bone). In opposition, the particles of Bonelike® are regular, approximately cylindrical with round contours, and more uniform in size. Both the round shape of these particles and their narrow size distribution can have adverse effects regarding inflammation [44]. Moreover, although most of the particles of both materials are larger than 150 μm, a fraction of particles around 15 μm (that can be attributed to fragments of primary particles, also visible in SEM) was detected in the sample of Bonelike® which can also be responsible for the intensification of the inflammatory response of this material (since the presence of very small particles tend to increase the risk of inflammatory reactions [45].

On the other hand, the surface characteristics of both materials are also distinct, being the Bonelike® granules more smooth, certainly as a consequence of their manufacturing process. This feature was confirmed by the result of the nitrogen adsorption method (Table 1) that revealed that Osteobiol® particles, though larger, possess a much larger specific surface area than those of Bonelike® (about 15 fold), which appears to be also an advantage in terms biological response [46].

Concerning porosity and pore size distribution (Table 1 and Figure 5), and besides the total porosity values being similar for both materials (≈ 50 %), the particles of Osteobiol® exhibit a higher amount of intraparticle pores (also visualized in the SEM pictures) typical of the cancellous bone fragments, which favor vascularization.

Another aspect investigated was the hydrophilicity/hydrophobicity natures of these materials since this parameter determine, in a great extent, the response of the host tissue, i.e. the immune and inflammatory response. Generally, hydrophilic surfaces induce milder responses compared to the ones set by hydrophobic surfaces [47]. Despite the experimental limitations resultant from measuring the contact angle in a powder material, both samples were found to be hydrophilic.

Finally, it is known that chemical composition can also greatly influence the cellular response [28]. The XRD and FTIR analysis of Bonelike® confirm that this material is composed of three crystalline phases: a major phase of HA and two secondary phases of α-TCP and β-TCP, in accordance with the literature [33, 48]. On the contrary, the XRD spectrum of Osteobiol® (Figure 6b) indicates a low-crystallinity material, in agreement with its constitution: a crystalline phase (carbonated hydroxyapatite) and an amorphous phase (collagen). As it has been reported, composites of HA and TCP induce greater initial inflammatory responses compared with HA alone [49], which could help to justify the more intense inflammation reaction of Bonelike® implant.

Also the Ca/P ratio is reported to have an impact on material degradation [49], as it affects particles solubility (and consequently ion release). Although, theoretically, the Ca/P ratio of Bonelike® should lie between 1.5 and 1.67 (the Ca/P ratio of α- and β-TCP and the Ca/P ratio of HA, respectively), slightly lower experimental values were obtained by EDS (1.35 ± 0.07). As for Osteobiol®, the Ca/P ratio reported by the producers is 1.73 (37), which is in agreement with the measured value (1.75±0.16). The lower Ca/P ratio of Bonelike® indicates that this material is more prone to degradation [50]. However this may not be relevant in the present case considering the short evaluation period (one week).

In conclusion, the thorough characterization of these materials revealed substantial differences in their physico-chemical properties that seem to explain, at least partly, the more intense inflammatory response of Bonelike®. However, it should be, once again, stressed that only the initial inflammatory response was of interest to this study and thus neither the immune response nor bone regeneration were evaluated. In fact, the next stages of the work will be to identify the immune mediators involved in the process, particularly cytokines and chemokines, being the final goal to search for an inflammatory profile of each biomaterial tested.

5. Conclusion

The extensive characterization of the graft materials Bonelike® and Osteobiol® performed in this work revealed that these two commercial bone grafts, although used in the clinical practice for the same purposes, possess markedly different properties either chemical (e.g., composition, crystallinity, Ca/P ratio) and physical (e.g., particle size and shape, surface area, density and pore size distribution). It is thus not surprising to find out that they induce different inflammatory responses after one week

implantation. In fact, in this study, it was detected that the tissue response elicited by Bonelike® granules was consistently more intense than that triggered by Osteobiol® granules, particularly in terms of collagen production and formation of fibrous capsule. The differences found in the explored characteristics seem to justify this distinct *in vivo* performance. It is believed the provided data will assist clinicians to make a more informed choice between these two materials.

References

[1] A. Stavropoulos, P. Windisch, D. Szendroi-Kiss, R. Peter, I. Gera, A. Sculean, J. Periodontol. 81 (2010) 325-334.

[2] N. Baldini, M. De Sanctis, M. Ferrari, Dent. Mater. 27 (2011) 61-70.

[3] J.D. Bashutski, H.L. Wang, J. Endod. 35 (2009) 321-328.

[4] P. Windisch, D. Szendroi-Kiss, A. Horvath, Z. Suba, I. Gera, A. Sculean, Clin. Oral Investig. 12 (2008) 257-264.

[5] S.L. Oh, A.F. Fouad, S.H. Park, J. Endod. 35 (2009) 1331-1336.

[6] J. Ferri, J. Dujoncquoy, J.M. Carneiro, G. Raoul, Head Face Med. 4 (2008) 31.

[7] S. Sakka, C. Krenkel, J. Craniomaxillofac. Surg. 39 (2011) 187-191.

[8] L. Lin, M.Y. Chen, D. Ricucci, P.A. Rosenberg, J. Endod. 36 (2010) 618-625.

[9] P. Sreedevi, N. Varghese, J.M. Varugheese, J. Conserv. Dent. 14 (2011) 68-72.

[10] T. Arx, M. AlSaeed, Saudi Dental J. 23 (2011) 113-127.

[11] J. Handschel, M. Simonowska, C. Naujoks, R.A. Depprich, M.A. Ommerborn, U. Meyer, N.R. Kübler, Head Face Med. 5 (2009) 12.

[12] R.A. Depprich, J.G. Handschel, C. Naujoks, T. Hahn, U. Meyer, N.R. Kubler, Head Face Med. 3 (2007) 2.

[13] D. Tadic, M. Epple, Biomaterials 25 (2004) 987-994.

[14] H. Masago, Y. Shibuya, S. Munemoto, J. Takeuchi, M. Umeda, T. Komori, Y. Kuboki, Kobe J. Med. Sci. 53 (2007) 257-263.

[15] J.A. McAuliffe, J. Hand Ther. 16 (2003) 180-187.

[16] D.I. Ilan, Operat. Tech. Plast. Reconstr. Surg. 9 (2002) 151-160.

[17] P.V. Giannoudis, H. Dinopoulos, E. Tsiridis, Injury 36 (2005) S20-27.

[18] S. Catros, F. Guillemot, E. Lebraud, C. Chanseau, S. Perez, R. Bareille, J. Amédeé, J.C. Fricain, IRBM 31 (2010) 226-233.

[19] A.C. da Cruz, M.T. Pochapski, J.B. Daher, J.C. da Silva, G.L. Pilatti, F.A. Santos, J. Oral Sci. 48 (2006) 219-226.

[20] S.N. Parikh, J. Postgrad. Med. 48 (2002) 142-148.

[21] J. Van der Stok, E.M. Van Lieshout, Y. El-Massoudi, G.H. Van Kralingen, P. Patka, Acta Biomater. 7 (2011) 739-750.

[22] J.M. Anderson, Annu. Rev. Mater. Res. 31 (2001) 81-110.

[23] S. Allegrini Jr., B. Koening Jr., M.R. Allegrini, M. Yoshimoto, T. Gedrange, J. Fanghaenel, M. Lipski, Ann. Acad. Med. Stetin. 54 (2008) 70-81.

[24] K.M. Nuss, B. von Rechenberg, Open Orthop. J. 2 (2008) 66-78.

[25] D.F. Williams, Biomaterials 29 (2008) 2941-2953.

[26] M. Figueiredo, J. Henriques, G. Martins, F. Guerra, F. Judas, H. Figueiredo, J. Biomed. Mater. Res. B Appl. Biomater. 92 (2010) 409-419.

[27] A. Tampieri, G. Celotti, S. Sprio, A. Delcogliano, S. Franzese, Biomaterials 22 (2001) 1365-1370.

[28] N. Costa, B. Melo, R. Brito, G. Fernandes, V. Bernardo, E. Fonseca, M. Conza, G. Soares, J. Granjeiro, Mater. Res. 12 (2009) 245-251.

[29] S. Ghanaati, M. Barbeck, C. Orth, I. Willershausen, B.W. Thimm, C. Hoffmann, A. Rasic, R.A. Sader, R.E. Unger, F. Peters, C.J. Kirkpatrick, Acta Biomater. 6 (2010) 4476-4487.

[30] M. Ramirez-Fernandez, J.L. Calvo-Guirado, R.A. Delgado-Ruiz, J.E. Mate-Sanchez del Val, V. Vicente-Ortega, L. Meseguer-Olmos, Clin. Oral Implants Res. 22 (2011) 767-773.

[31] J.C. Knowles, G.W. Hastings, J.D Santos, Patent WO/2000/068164.

[32] M. Gutierres, M.A. Lopes, N. Sooraj Hussain, A.F. Lemos, J.M. Ferreira, A. Afonso, A.T. Cabral, L. Almeida, J.D. Santos, Acta Biomater. 4 (2008) 370-377.

[33] L.A. Prado da Silva, I.R Gibson, J.M.F Ferreira, J.D Santos, J. Non-Crys. Solids 304 (2002) 286-292.

[34] P.S. Gomes, J.D. Santos, M.H. Fernandes, Acta Biomater. 4 (2008) 630-637.

[35] M.A. Lopes, J.C. Knowles, J.D. Santos, Biomaterials 21 (2000) 1905-1910.

[36] J.D. Santos, M.A. Lopes, Bonelike graft for regenerative bone applications, in: M.J. Jackson, W. Ahmed (Eds.), Surface Engineered Surgical Tools and Medical Devices, Springer, New York, 2007, pp. 477-512.

[37] M.V. Thomas, D.A. Puleo, J. Dent. Res. 90 (2011) 1052-1061.

[38] D.H. El-Rouby, S.A. Abd-El-Halim, Egyptian Dental J. 55 (2009) 1-23.

[39] M. Figueiredo, A. Fernando, G. Martins, J. Freitas, F. Judas, H. Figueiredo, Ceram. Int. 36 (2010) 2383-2393.

[40] N. Matsumoto, K. Yoshida, K. Hashimoto, Y. Toda, Materials Res. Bull. 44 (2009) 1889-1894.

[41] M.C. Chang, J. Tanaka, Biomaterials 23 (2002) 4811-4818.

[42] A. Rapacz-Kmita, A. Ślósarczyk, Z. Paszkiewicz, C. Paluszkiewicz, J. Mol. Struct. 704 (2004) 333-340.

[43] J. Kolmas, M. Szwaja, W. Kolodziejski, J. Pharmaceut. Biomed. 61 (2012) 136-141.

[44] A. Grandjean-Laquerriere, P. Laquerriere, D. Laurent-Maquin, M. Guenounou, T.M. Phillips, Biomaterials 25 (2004) 5921-5927.

[45] P. Laquerriere, A. Grandjean-Laquerriere, E. Jallot, G. Balossier, P. Frayssinet, M. Guenounou, Biomaterials 24 (2003) 2739-2747.

[46] A. Grandjean-Laquerriere, P. Laquerriere, M. Guenounou, D. Laurent-Maquin, T.M. Phillips, Biomaterials 26 (2005) 2361-2369.

[47] B. Nilsson, K.N. Ekdahl, T.E. Mollnes, J.D. Lambris, Mol. Immunol. 44 (2007) 82-94.

[48] A.C. Queiroz, J.D. Santos, F.J. Monteiro, I.R. Gibson, J.C. Knowles, Biomaterials 22 (2001) 1393-1400.

[49] S. Ghanaati, M. Barbeck, R. Detsch, U. Deisinger, U. Hilbig, V. Rausch, R. Sader, R.E. Unger, G. Ziegler, C.J. Kirkpatrick, Biomed. Mater. 7 (2012) 015005.

[50] M.S. Laranjeira, A.G. Dias, J.D. Santos, M.H. Fernandes, Mater. Sci. Eng. C 29 (2009) 930-935.

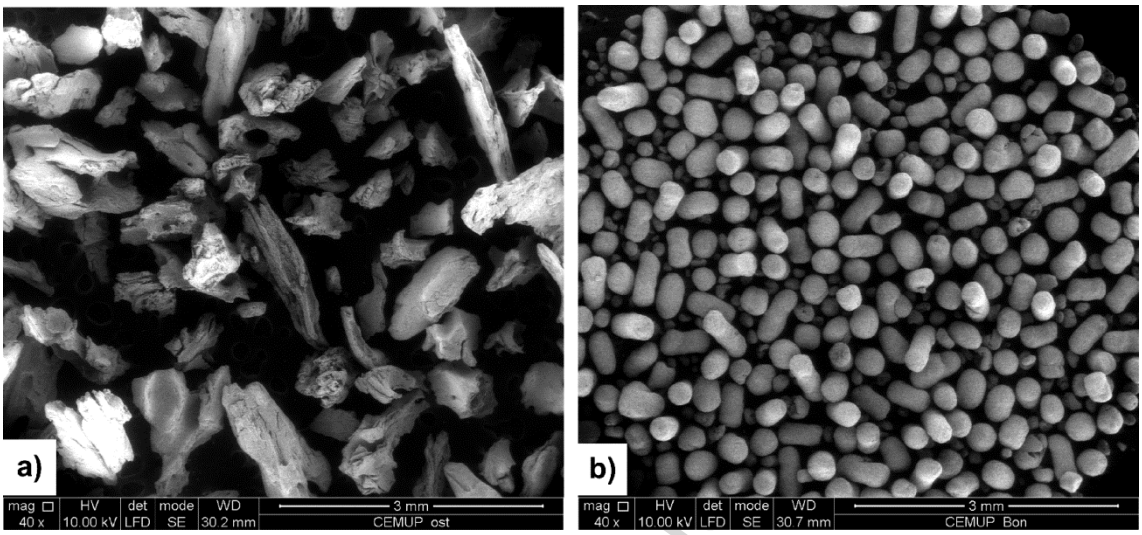

Figure 1

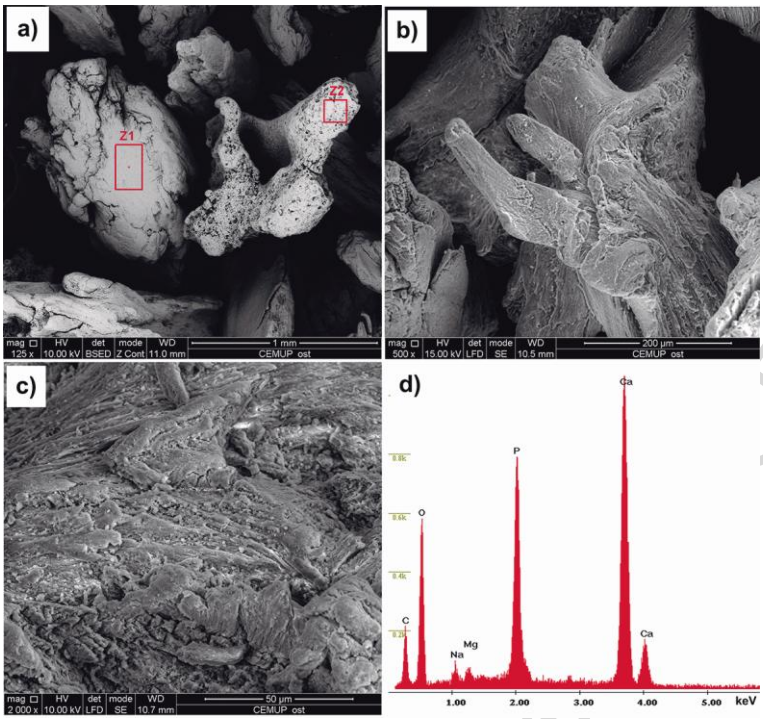

Figure 2

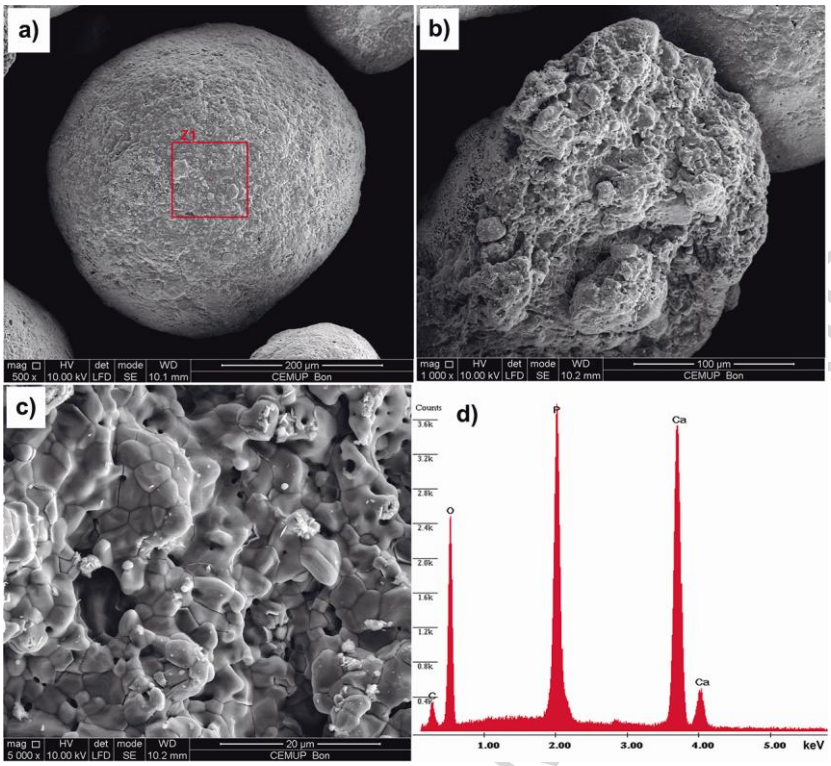

Figure 3

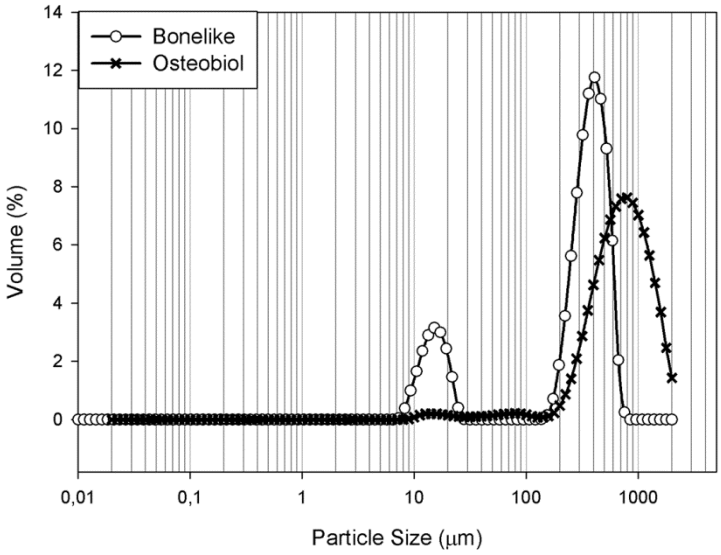

Figure 4

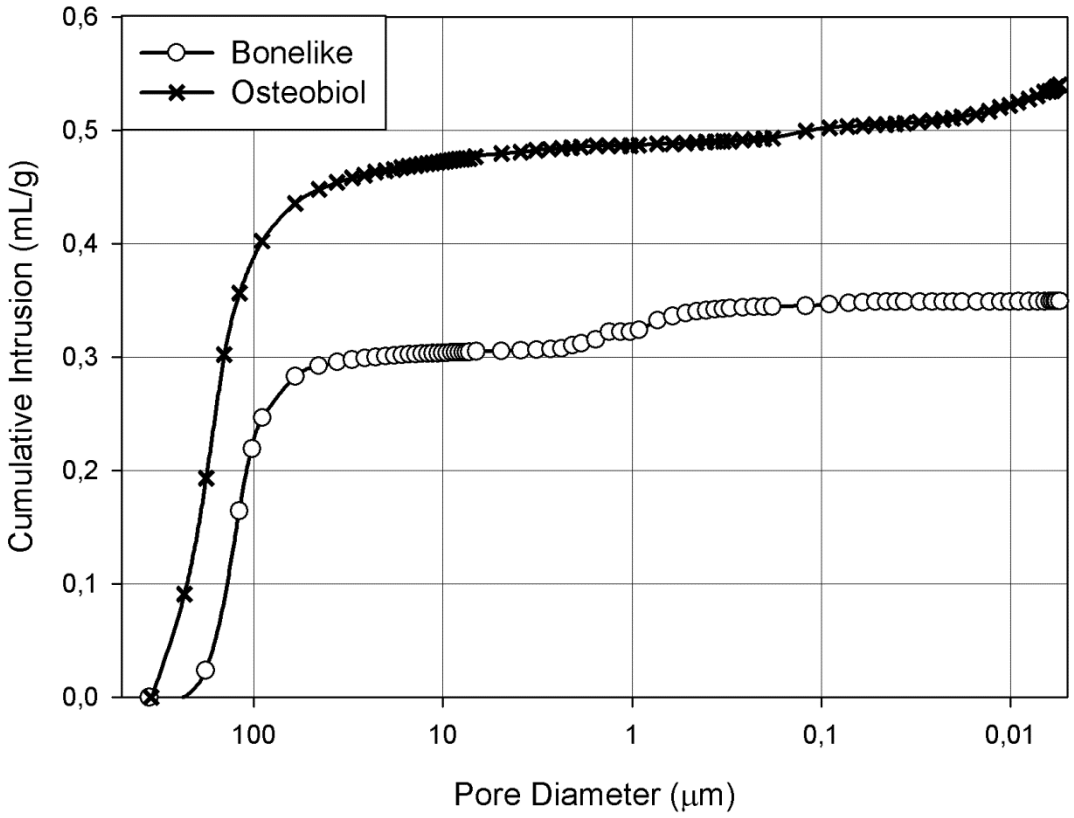

Figure 5

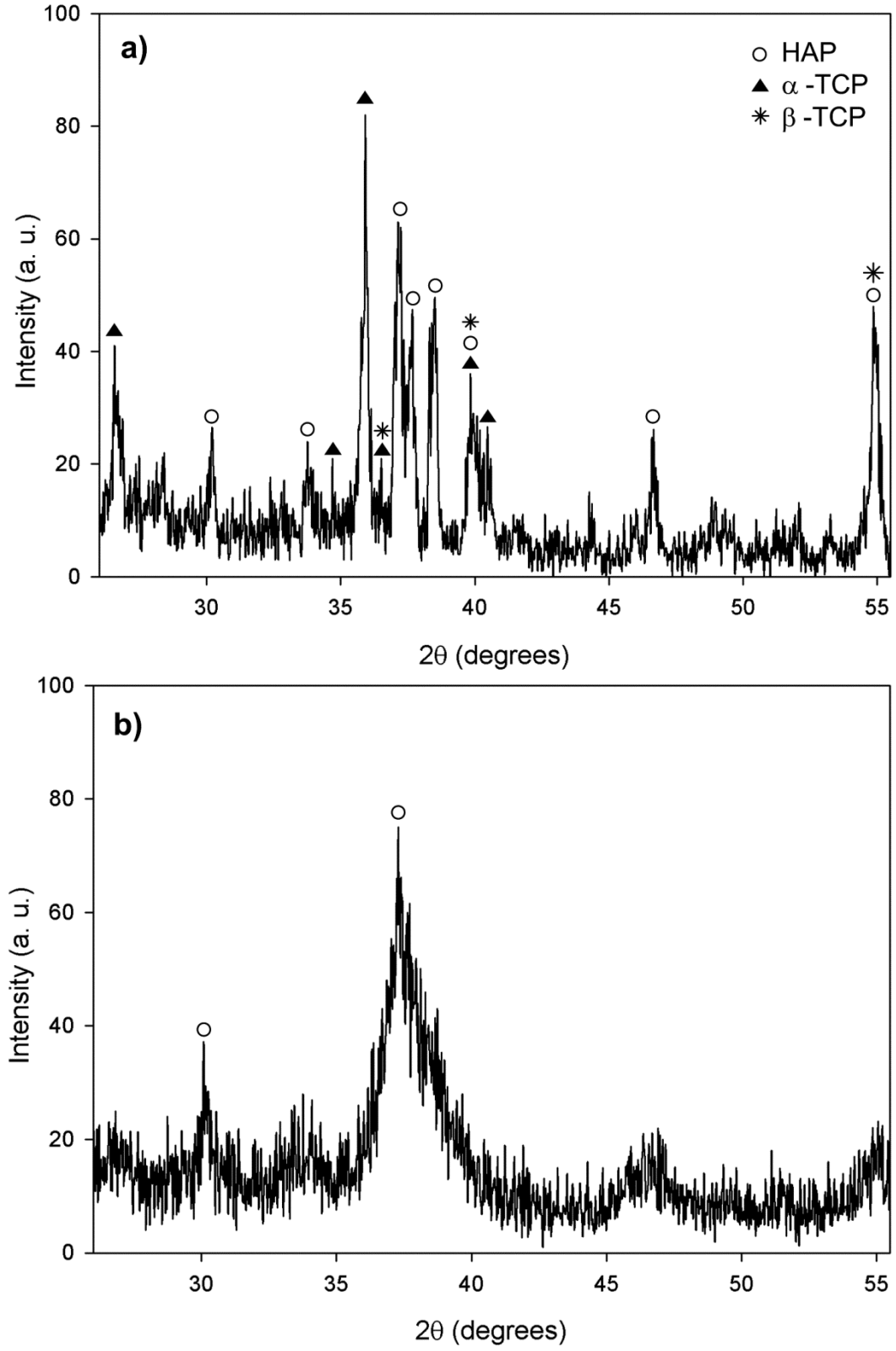

Figure 6

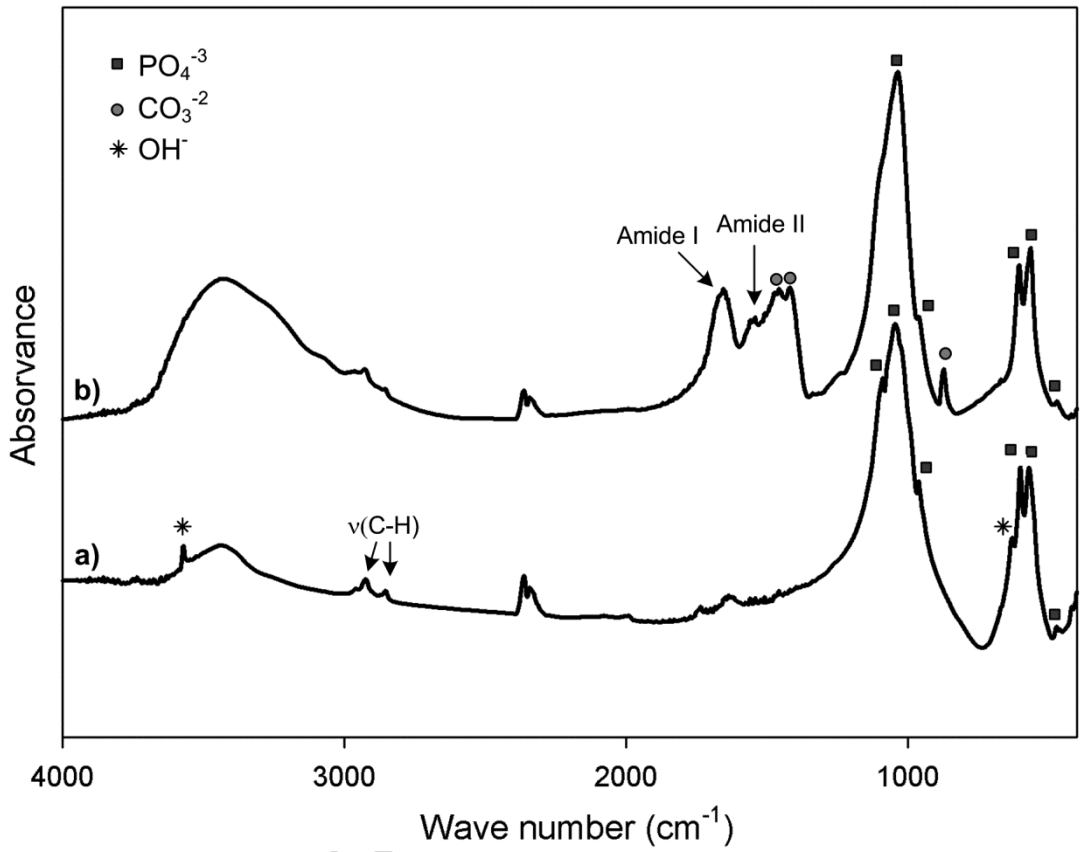

Figure 7

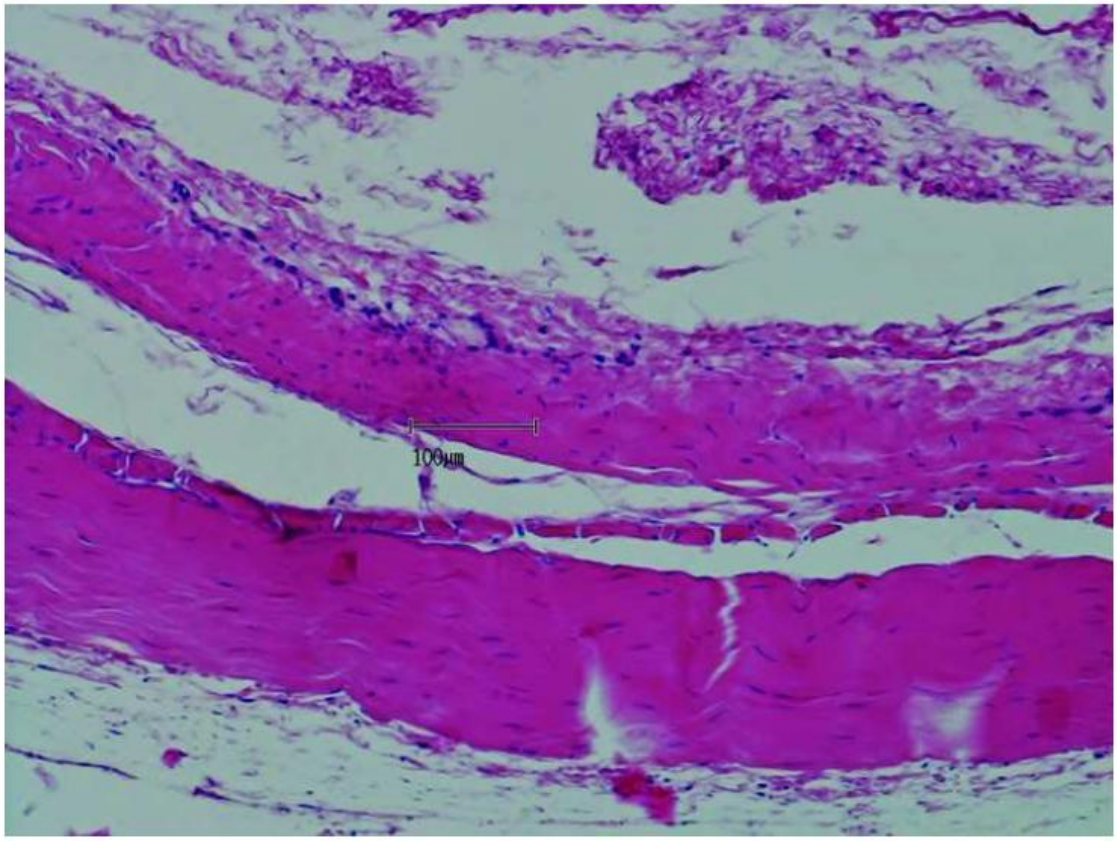

Figure 8

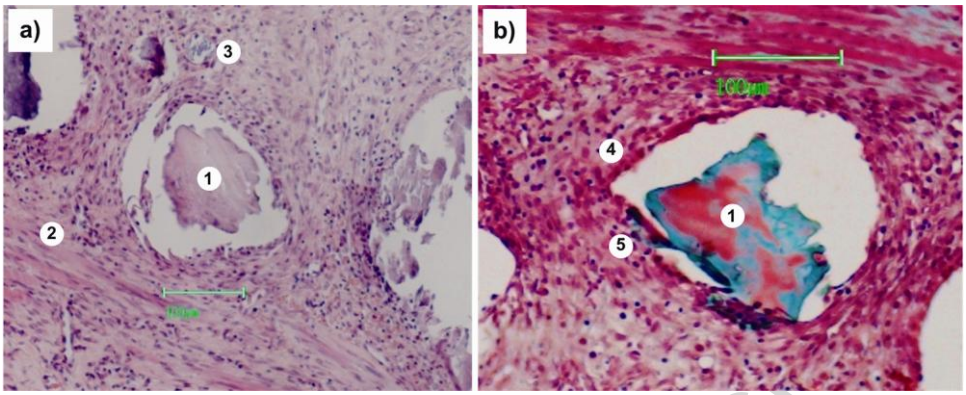

Figure 9

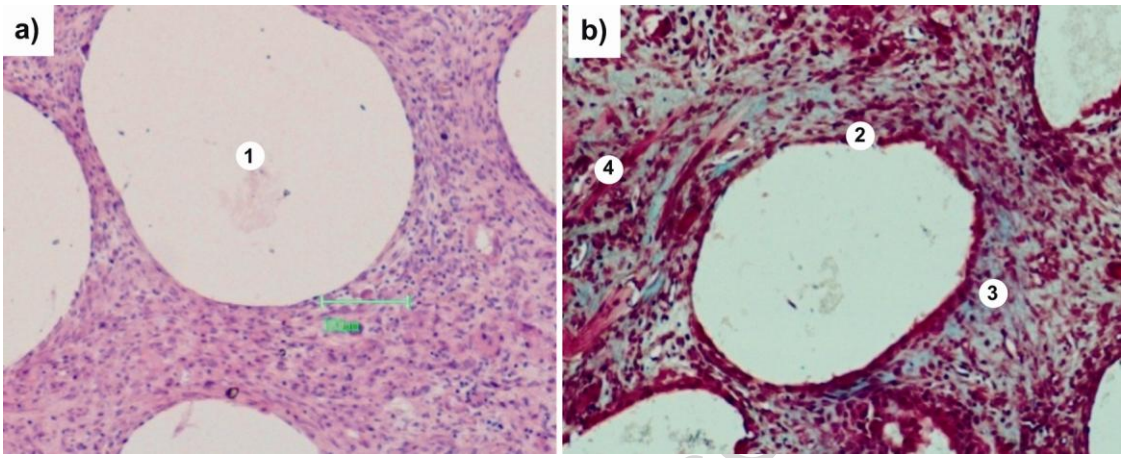

Figure 10

Figure legends

Figure 1. SEM micrographs of: a) Osteobiol®; b) Bonelike®; (40× magnifications).

Figure 2. Micrographs of Osteobiol® particles with different magnifications: a) 125x; b) 500x; c) 2000× and a representative EDS spectrum (d).

Figure 3. Micrographs of Bonelike® particles with different magnifications: a) 500x; b) 1000x; c) 5000x and a representative EDS spectrum (d).

Figure 4. Particle size distribution of Bonelike® and Osteobiol® measured by laser diffraction spectrometry. As illustrated, a very small fraction of particles of Osteobiol, could not be measured, as they exceeded the upper limit of the instrument (2 mm).

Figure 5. Mercury intrusion cumulative curves of Bonelike® and Osteobiol®. The intrusion profile of both materials show a considerable intrusion in pores between 400 µm and approximately 50 µm, corresponding mainly to the filling of the spaces between the particles (the so called "interstices" or "interparticle" spaces), followed by a much attenuated mercury penetration in smaller pores ("intraparticle" pores). For Bonelike®, no mercury intrusion was found between 50 µm and about 3 µm, but a small intrusion was detected in the interval 3 - 0.7 µm. No significant intrusion was found afterwards. As for the Osteobiol®, a small but approximately constant mercury intrusion with increasing pressure was found below 50 µm, denoting the presence of pores within this size range.

Figure 6. Diffractograms of: a) Bonelike®; b) Osteobiol®. Diffraction peaks assign to: (○) Hydroxyapatite (JCPDS nº 09-432); (△) α-Tricalcium phosphate (JCPDS nº 29-0359); (✸) β- tricalcium phosphate (JCPDS nº 86-1585).

Figure 7. FTIR spectra of: a) Bonelike®; b) Osteobiol®.

Figure 8. Representative image of optical microscope histological section of the sham group from mice implanted with saline. There is evidence of muscle fibers disrupted due to the injection procedure, but inflammatory cells are absent (magnification of 20x).

Figure 9. Representative images of optical microscope histological sections of implantation bed of Osteobiol®. a) HE staining: 1. implant particle involved by inflammatory infiltrate showing granulation tissue rich in mononuclear cells. 2. muscle fibers disrupted due the injection procedure of the biomaterial granules. 3. blood vessel with some red cells; b) TM staining: 1. implant particle. 4. capsule formed around the implant particle. 5. collagen fibers stained in green.

Figure 10. Representative images of optical microscope histological sections of implantation bed of Bonelike®. a) HE staining: 1. implant particle (missing) surrounded by inflammatory infiltrate rich in mononuclear cells; b) TM staining: 2. capsule formed around the implant particle. 3. collagen fibers stained in green. 4. fibroblasts area.

Table 1. Particle size distribution, specific surface area, porosity, and density of Osteobiol® and Bonelike® granules.

Technique	Obtained information	Parameters	Osteobiol®	Bonelike®
Laser Diffraction	Particles size distribution[a]	D_{10} (µm)	298	14.3
		D_{50} (µm)	672	326
		D_{90} (µm)	1330	510
Nitrogen Adsorption	Surface area	Specific surface area ($m^2\ g^{-1}$)	9.404	0.636
Mercury Intrusion Porosiometry	Pore size distribution, porosity	Intruded volume ($cm^3 g^{-1}$)	0.54	0.35
		Intruded volume in pores smaller than 10 µm ($cm^3 g^{-1}$)	0.068	0.046
		Porosity[b] (%)	53	48
		Skeletal Density[c] ($g\ cm^{-3}$)	2.11	2.69
Helium Pycnometry	Density	Real density ($g\ cm^{-3}$)	2.39±0.03	2.77±0.05

[a] D_{10}, D_{50}, D_{90} - particle diameters corresponding to 10, 50 and 90 %, respectively, of the cumulative size distribution curve.
[b] Corresponding to pores < 400 µm.
[c] Calculated based on the volume of mercury intruded at the maximum pressure (2000 atm).

Table 2. Scores obtained for the reparative process triggered by each graft material (0 (absent), 1 (moderate) and 2 (high)).

Parameter/Biomaterial	Osteobiol®	Bonelike®
Fibrosis	1	2
Hemorrhage	0	0
Collagen	1	2
Vascularization	1	1
Capsule thickness	1	2

Highlights

- Two commercial bone grafts - Bonelike® and Osteobio®- were characterized
- *In vivo* inflammatory response was evaluated after 1 week implantation
- Both materials did not cause severe inflammation
- Nevertheless, Bonelike elicit a consistently more intense inflammatory response